Journal of Ceramic Processing Research. Vol. 21, No. 5, pp. 579~585 (2020)
(Received 1 May 2020, Received in revised form 19 June 2020, Accepted 16 July 2020)
https://doi.org/10.36410/jcpr.2020.21.5.579

J O U R N A L O F
Ceramic
Processing Research

Effects of NH_3 pre-treatment time on nitrogen-polar GaN grown on carbon-face 4H-SiC using high-temperature metal-organic chemical vapor deposition

Minho Kim[a], Uiho Choi[a], Kyeongjae Lee[a], Donghyeop Jung[a], Taemyung Kwak[a], Byeongchan So[a], KapRyeol Ku[b] and Okhyun Nam[a,*]

[a]*Nano-Optical Engineering, Korea Polytechnic University (KPU), Siheung, Gyeonggi 427-793, Republic of Korea*
[b]*SKC Advanced Technology R&D Center, #12, Jeongja-ro, Jangan-hu, Suwon-Si, Gyeonggi-do, Republic of Korea*

We investigated the effects of NH_3 pretreatment time on N-polar GaN grown on 4° off-cut C-face 4H-SiC using high temperature metal-organic chemical vapor deposition. The NH_3 pre-treatment time was changed from 2 to 32 minutes at 1,350 °C. The polarity of layer was confirmed by aqueous KOH etching method. As the NH_3 treatment time increased, the etch rate of the layer was increased and the structural and optical properties were deteriorated. The total hillock density of samples was 7.5, 12.9, and 25.1 × 10^2 cm^{-2} respectively. Furthermore, we compared the luminescence spectra of Ga-polar and N-polar GaN films using low-temperature photo-luminescence measurement. The N-polar GaN layer showed Y1 peak (3.45 eV), which is attributed to the existence of inversion domain boundary (IDB) in the layer.

Keywords: Epitaxy; Metalorganic chemical vapor deposition; Gallium nitride; Nitrogen polar; Pre-treatment

Introduction

GaN, is one of the most promising materials for future electronics industry because of its wide bandgap and tunability, high thermal and chemical stability, and high critical electric field and saturated velocity, has been widely utilized for various applications such as light-emitting diodes, laser diodes as well as high power and high-frequency transistors. When GaN is grown on sapphire or SiC substrates by MOCVD, the film has typically the (0001) orientation corresponding to the Ga-face. Therefore, most GaN-based device applications have been fabricated with GaN having a gallium polarity [1-4]. In recent years, however, GaN films with a nitrogen face have gained attention because they offer several advantages over Ga-polar GaN [5, 6]. For example, when HEMT is grown in the N-polar direction, the polarization field orientation is flipped over from that of the Ga-polar direction. Therefore, the N-polar based HEMT structure has a natural back-barrier because an AlGaN or AlN barrier is formed beneath the GaN channel [6]. This barrier prevents a two-dimensional electron gas (2DEG) from spilling over toward the buffer layer and acts as a back-barrier in double-heterostructure HEMT grown into Ga-polar. In addition, N-polar structure can be achieved very low ohmic contact resistance by contacting lower bandgap material (i.e. GaN) unlike Ga-face. Consequently, the N-polar GaN-based HEMT structure is efficient for suppressing the short channel effects with the N-polar GaN-based RF device providing a superior high-frequency performance compared to normal Ga-polar based devices [7, 8]. In addition, the N-polar GaN also has several advantages for green LEDs. For example, it is possible to grow InGaN layer with high In mole fraction because N-polar surface has high InN stability [9]. Moreover, because N-polar GaN has a strong propensity for p-doping than Ga-polar GaN, it can be said that N-polar GaN is more useful in the design of electronic and optical devices [5].

Although there are many theoretical and experimental benefits to N-polar based devices, it is difficult to grow high-quality N-polar GaN films having a smooth surface because of the defect formation such as hillocks, inversion domains, surface undulations, etc [5, 10, 11]. Based on previous research on N-polar GaN growth, it was found that the condition of the substrate pretreatment is essential for high-quality film growth [12]. We have also previously noted the importance of the NH_3 pretreatment temperature under nitrogen-rich conditions [11]. In particular, we found that the N-polar GaN film quality improved as the NH_3 pretreatment temperature increased. Based on our experiments, the optimum treatment temperature was 1,350 °C [11]. In this paper, we investigated the effect of NH_3 pretreatment time on N-polar GaN film grown on C-face 4H-SiC using high-temperature metalorganic chemical vapor deposition (HT-MOCVD).

*Corresponding author:
Tel : +82-31-8041-0718
Fax: +82-31-8041-0729
E-mail: ohnam@kpu.ac.kr

Experimental Details

2”× 6 HT-MOCVD was utilized for all growth experiments. TaC coated SiC susceptor was used for high-temperature (above 1,100 ºC) condition. For the growth of N-polar GaN films, 4º off-cut C-face (000-1) 4H-SiC substrates were prepared and organic residues were cleaned with acetone and isopropyl-alcohol for 10 min. All the 4º off-cut C-face (000-1) 4H-SiC substrates were provided by SKC solmics Co., Ltd. (SKC). Subsequently, it was rinsed with deionized water for 3 mins and dried by nitrogen (N_2) gas. Hydrogen (H_2), trimethyl gallium (TMGa), trimethyl aluminum (TMAl), and ammonia (NH_3) were used as a carrier gas and the precursors, respectively. The pre-treatment time using NH_3 was changed to 2, 16, and 30 min for sample A, B, and C, respectively, and the temperature was set at 1,350 ºC. Previously, it was found that the optimum treatment temperature in our MOCVD system for growth of the N-polar GaN on SiC was 1,350 ºC [11]. The temperature profile of the sample growth is shown in Fig. 1(a). First, the SiC substrate was loaded into the reactor. The air was removed and substituted with N_2 for H_2 injection. Next, the substrate was heated to 1,100 ºC for thermal cleaning of organic residues using H2. The temperature was then increased to 1,350 ºC for NH_3 surface treatment, varying from 2 to 32 min. After that, the ~25 nm-thick AlN nucleation layer (NL) was grown on the SiC substrate. Finally, the 2 μm-thick GaN layer was grown on the AlN NL. The detailed description of the sample growth conditions was addressed elsewhere [11]. The sample structure is shown in Fig. 1(b). The polarity of the grown layer was verified using 0.45M potassium hydroxide (KOH) aqueous solution at 80 ºC for 5 min, and it was confirmed that the layer successfully grew into nitrogen polarity [11]. In addition, Ga-polar GaN sample was also grown on on-axis Si-face SiC using the growth condition of sample A to compare epi-layer characteristics. The scanning transmission electron microscopy high-angle annular dark-field imaging (STEM-HADDF, JEM-2100F with Cs corrector, JEOL/CEOS) with 200 keV accelerating voltages was utilized to verify the structural property of the epitaxially grown layer at the interface. Using focused ion beam (FEI, Quanta 3D FEG), 70-nm-thick samples were prepared for the TEM measurement. The optical microscopy (Nikon, Eclipse LV 150), the field-emission scanning electron microscopy (Hitachi, S-4000) with an accelerating voltage of 15 kV, the high resolution X-ray diffraction (Panalytical, X’Pert Pro), low-temperature photoluminescence system (Dongwoo optron) using 325 nm He-Cd laser (Kimmon) and liquid He cryostat, and the atomic force microscopy (Park systems, XE-7) with a non-contact mode were used for evaluating the hillock density, determining the etch rate, evaluating the crystallinities and structural properties, and measuring the surface roughness, respectively.

Results and Discussion

Three N-polar GaN samples with different pretreatment times of 2, 16, and 32 minutes, respectively, were grown HT-MOCVD, and TEM measurement was conducted to verify the structural property of sample A. Fig. 2(a) shows the selective area electron diffraction (SAED) pattern with zone axis $[10\text{-}10]_{SiC}$ of N-polar GaN/AlN NL/SiC structure indicating that the epi-layer structure was successfully grown. The electron diffraction area was carefully selected by focusing on the GaN/AlN interface. It was observed that the diffracted patterns overlapped each other owing to the very similar lattice constants between GaN and AlN [13]. However, in the case of farther points from center, reciprocal lattice points (RLPs) can be distinguished in reciprocal space due to the smaller d-spacing. The two RLPs in the third position vertically measured distances of ~11.777 and ~11.404 nm^{-1}, respectively. In other words, the d-spacing of each point is 0.085 and 0.088 nm, respectively. These values were consistent with the one-sixth of lattice constant values of AlN and GaN

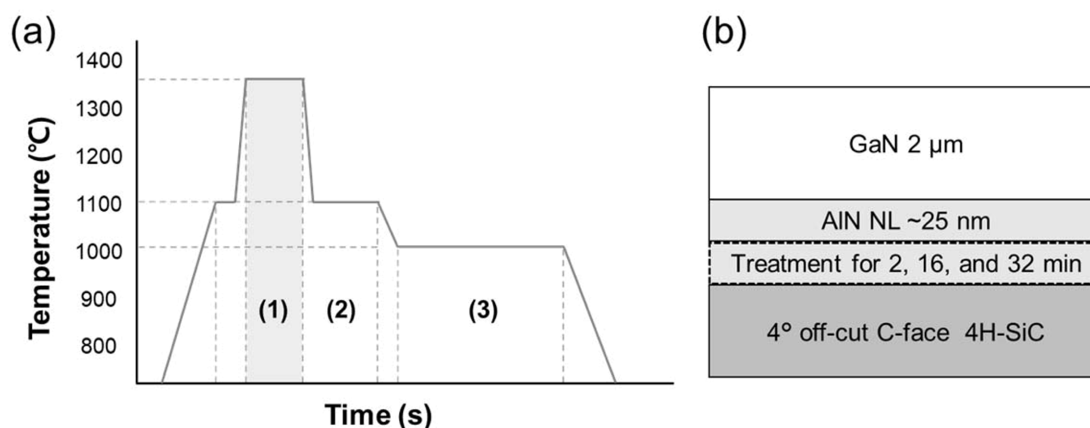

Fig. 1. (a) Temperature profiles (1) NH_3 pre-treatment at 1,350 ºC for 2, 16, and 32 min of sample A, B and C, respectively, (2) AlN nucleation layer growth, and (3) GaN growth step. (b) schematic image of sample structure.

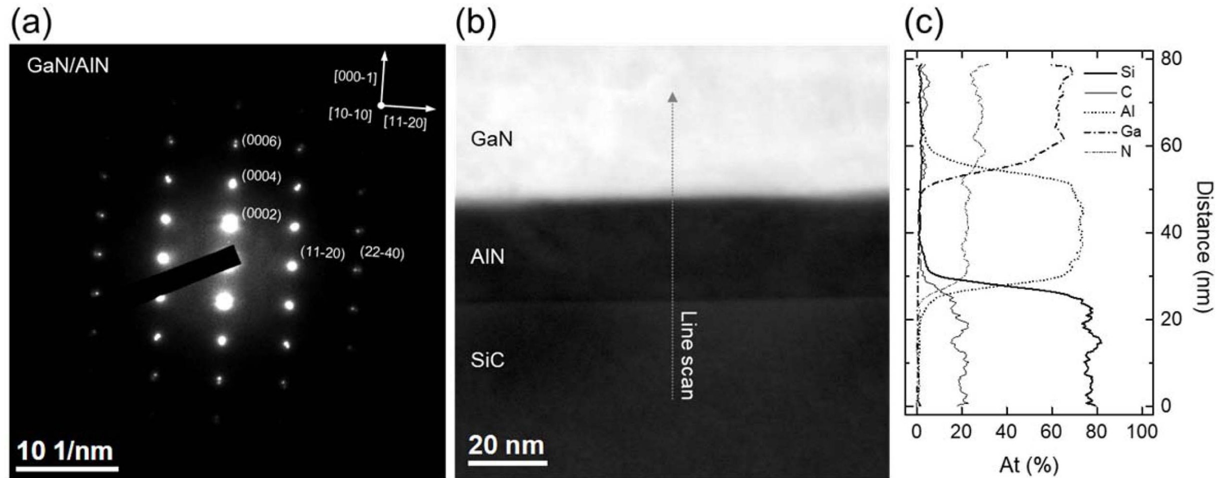

Fig. 2. (a) SAED pattern of GaN/AlN structure with zone axis of [10-10], (b) STEM image, and (c) EDX line scan profile of N-polar GaN/AlN/C-face SiC structure.

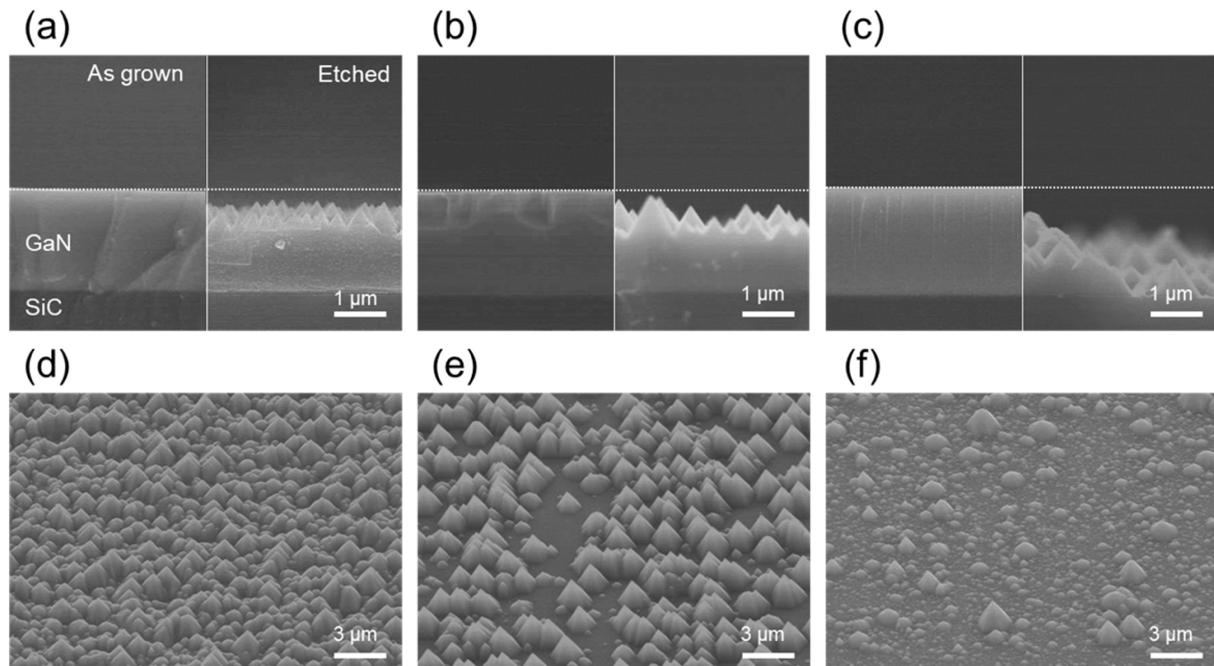

Fig. 3. Cross-sectional SEM images (15k magnification) of as grown and KOH etched GaN layers after NH_3 treatment for 2 (a), 16 (b), and 32 min (c), and bird's eye view images (5k magnification) of KOH etched GaN layer after NH_3 treatment for 2 (d), 16 (e), and 32 min (f).

(c_{AlN} = 4.98 Å, c_{GaN} = 5.185 Å) while also having an error of just below 2% [13]. These TEM measurement results were in good agreement with the XRD results (not shown here). Therefore, it can be concluded that was reasonable to say that these RLPs are the diffracted points of the epitaxially grown AlN and GaN layers. In the same manner, the second RLPs in the horizontal direction measured the distances of ~12.580 and ~12.477 nm^{-1}, respectively. That is, the d-spacings are 0.078 and 0.080 nm, respectively, which are identical values with the d-spacing of the AlN and GaN (22-40) planes. Therefore, it can be said that the epitaxial relationship of the GaN/AlN/SiC structure is $(000\text{-}1)_{GaN}$ // $(000\text{-}1)_{AlN}$ // $(000\text{-}1)_{SiC}$ and $[11\text{-}20]_{GaN}$ // $[11\text{-}20]_{AlN}$ // $[11\text{-}20]_{SiC}$. Next, for the compositional analysis, line profile of Energy-dispersive X-ray spectroscopy (EDX) was obtained as shown in Fig. 2(b) and (c). The STEM-HADDF image of the GaN/AlN/SiC structure (Fig. 2(b)) shows that the AlN NL thickness is approximately 25 nm. Meanwhile, Fig. 2(c) shows the line scan profile of GaN/AlN/SiC structure indicating the sharp interface between them. The reason for the low atomic percentage of light elements such as carbon and nitrogen can be attributed to poor signal generation and damage caused by accelerated electrons [14].

Fig. 3(a), (b), and (c) show the SEM cross-section images (15k magnification) of sample A, B, and C before and after KOH wet etching, respectively. The

cross-section images show that the thicknesses of all samples were identical at 2 μm KOH etched SEM image shows the triangular shaped pyramids having the {11-10} plane which are verifying the N-polarity of the samples [11]. It is worthy to note that the etched depth of each sample differed with NH_3 treatment time. This could be because the more defective layers were etched deeper. However, it was shown that no difference was observed before and after etching of the reference sample (not shown). Fig. 3(d), (e), and (f) show the bird's eye view images (5k magnification) of the wide surface area of etched samples. The surface coverage of N-polar hexagonal hillock residue roughly decreased as the NH_3 treatment time was increased.

The measured etch rates are shown in Fig. 4(a). The etched depth was obtained by averaging the peak and valley distances of the hexagonal hillock from the surface of the as-grown samples. The etch rate of sample A, B, and C was ~100, ~130, and ~270 nm/min, respectively. Fig. 4(b) shows the XRC FWHM trend for (002) and (102) planes of sample A, B, and C. It was found that the FWHMs of (002) and (102) planes of sample A, B, and C were 370 and 420, 440 and 500, as well as 470 and 610 arcsec, respectively (Table 1). For reference sample, the FWHMs of each plane were 130 and 200 arcsec, and these results confirm the high crystal quality of the Ga-polar GaN layer.

Fig. 5 shows the AFM scan results (20 × 20 μm^2) of sample A, B, and C. The root mean square (RMS) roughness of each sample was 13.37, 7.28, 5.64 nm, respectively as listed in Table 1. The surface flatness improved as treatment time was increased. This can be due to the well-defined step-terrace structure with increased treatment time, thus promoting step flow growth [12, 15, 16].

However, this result contradicted the trend of XRC FWHMs. The trade-off between crystal quality and surface roughness has been extensively discussed in previous studies [17, 18]. Although increased treatment time promotes the step-flow growth mode of the N-polar GaN layer, it should be noted that an excessively long treatment time could cause unintentional reaction with the substrate, potentially causing surface damage. For example, nitrogen in NH_3 bonds easily to Si atoms at the surface forming not only silicon nitride, but also silicon oxynitride when reacting with oxygen [19]. As oxygen atom is one of the reasons for inverted polarity resulting in inversion domain boundary (IDB) of N-

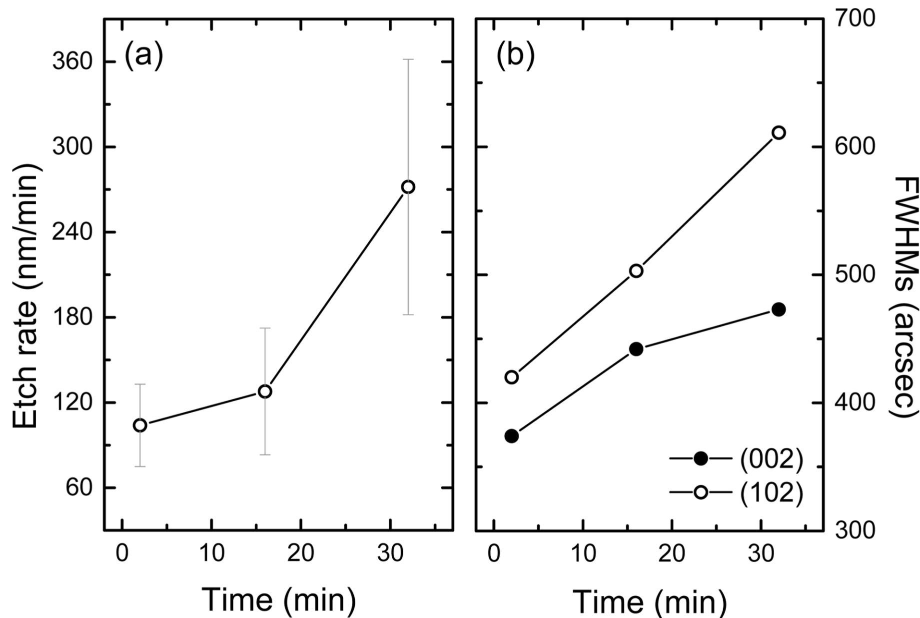

Fig. 4. Etch rate of N-polar GaN using aqueous KOH (a) and XRC FWHMs of N-polar GaN layer with different treatment time (b).

Table 1. XRC FWHMs, hillock density, surface RMS roughness, and PL I_{IDB}/I_{D0X} ratio of sample A, B, and C with different treatment time.

Sample		NH_3 treatment		XRC FWHM (arcsec)		Hillock density ($\times 10^2$ cm^{-2})			RMS roughness (nm)	I_{IDB}/I_{D0X} ratio
		Temperature (°C)	Time (min)	(002)	(102)	IDB-related	Step-related	Total		
Reference	(Ga-polar)		2	130	200	-	-	-	1.39	-
A		1350	2	370	420	0.8	6.7	7.5	13.37	1.52
B	(N-polar)		16	440	500	2.8	10.1	12.9	7.28	2.61
C			32	470	610	4.7	20.4	25.1	5.64	3.53

polar nitride film, the oxygen atoms in silicon oxynitride film at the surface would lead to formation of the IDB [20]. In our study, this assumption is the likely scenario, as the density of the IDB-related hexagonal increased with treatment time. The density of hexagonal hillock of sample A, B, and C were 0.8, 2.8, and 4.7×10^2 cm^{-2}, respectively (Table 1). In addition, Akiyama et al. reported that the rapid change of the surface morphology

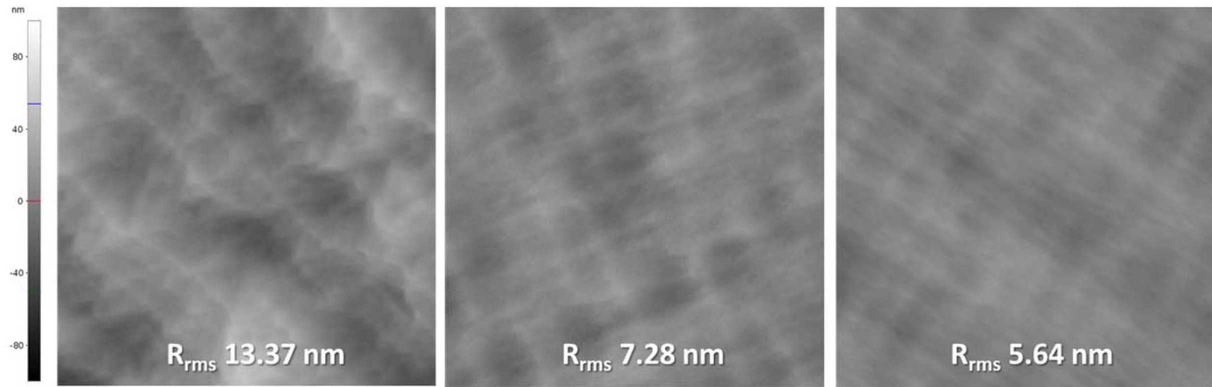

Fig. 5. AFM scan images (scan area 20×20 μm^2) of sample A (a), B (b), and C (c)..

Fig. 6. Stacked LT-PL spectra of reference, sample A, B, and C ((a)-(d)) with grating/blaze 300/500 nm. The enlarged spectra of reference and all samples (e) with grating/blaze 1200/250 nm. The inset OM image in (e) shows IDB-related hexagonal hillock of sample A (White arrows) and scale bar is 50 μm. Measurement temperature (T) was 11K and laser excitation power (Pexc) was 4.8 kW/cm^2, respectively.

of the 6H-SiC substrate starts at 1,250 ºC under hydrogen atmosphere because SiC vaporized as SiH_x and CH_y due to the reaction between SiC and H_2 [21]. Moreover, Zhang et al. reported the effects of treatment time on the surface morphology of the c-sapphire substrate showing that longer treatment time had deteriorated the surface morphology [22]. The altered terrace structure may affect the step-related hillock formation due to its sensitivity to surface morphology [10]. Similar to IDB-related hillock, the density of the step-related trigonal hillock also increased with treatment time. The density of trigonal hillock of each sample was 6.7, 10.1, and 20.4×10^2 cm^{-2}, respectively. That is, the total hillock density increased with the increase in treatment time. The hillock density results do not match with the trend in surface roughness results. It can be suggested that a longer treatment time improves the overall terrace structure of the substrate but deteriorates in partial regions. Meanwhile, the reference sample has RMS roughness of 1.39 nm, which is smoother than that of N-polar GaN. Moreover, there was no evidence of hillocks or surface defects observed.

To investigate the optical properties of sample A, B, and C, The LT-PL measurement was conducted at 11K. And Ga-polar GaN grown on Si-face SiC was also measured at same condition. The laser power and diameter was 13.7 mW and 20 μm. Figure 6 shows the stacked LT-PL spectra and enlarged spectra. According to the stacked LT-PL spectra, broad blue luminescence (BL) and yellow luminescence (YL) peaks were observed on all samples. BL band having interference pattern on reference sample means transitions from the conduction band or a shallow donor to a relatively deep acceptor [23]. or high quality GaN films at low temperature measurement. [24]. Fig. 6(e) shows the detailed spectra at near-band edge emission. The D^0X peak is the dominant emission at near 3.48 eV in all samples including reference sample. In case of reference sample, free-exciton peak that is shown at high quality films is observed beside the D^0X peak. The slight D^0X peak shift between reference and N-polar GaN sample series could be due to difference in substrate off-cut [25]. The D^0X-LO and 2LO peaks for the reference sample were clearly identified. Contrary to the reference sample, Y_1 (3.45 eV) peak was only detected in N-polar GaN samples indicating the existence of IDB in the film [26]. Hexagonal hillock (white arrow) is in inset optical microscope image, which is result of difference growth rate between Ga-polar and N-polar [27]. The ratio of integrated intensities of I_{IDB}/I_{D0X} for sample A, B, and C was 1.52, 2.61, and 3.53 respectively. The intensity of these peaks was in accordance with the density of the hexagonal hillock.

Conclusion

In conclusion, the effect of NH_3 pretreatment time on N-polar GaN growth on 4º off-cut C-face 4H-SiC was investigated. We found that the NH_3 pre-treatment time affects the crystal quality. The Full width at half maximum (FWHM) of the (00-2) and (10-2) plane of samples A, B, and C was 370, 440, and 470 arcsec, and 420, 500, and 610 arcsec, respectively. The hillock density related IDB of samples A, B, and C was 0.8×10^2, 2.8×10^2, and 4.7×10^2, respectively, whereas the root-mean-square (RMS) roughness values showed the tendency of decrease such as 13.7, 7.28, and 5.64 nm, respectively. This result is believed that the step flow growth can be improved due to the well-defined step-terrace structure as the pre-treatment time increase. From the PL measurement, only the N-polar GaN showed the Y1 peak at 3.45 eV, which is due to IDB. The intensity of the Y1 peak is related to the hillock because it is proportional to the pretreatment time. we expect that this study offers a deeper understanding and a practical growth condition for control in N-polar GaN epitaxy by applying NH_3 pre-treatment time.

Acknowledgments

This work was supported by Civil-Military Technology Cooperation Program 17-CM-MA-03

References

1. S. Pimputkar, J.S. Speck, S.P. Denbaars, and S. Nakamura, Nat. Photonics 3 (2009) 180-182.
2. S. Nakamura, M. Senoh, S.I. Nagahama, N. Iwasa, T. Yamada, T. Matsushita, H. Kiyoku, Y. Sugimoto, T. Kozaki, H. Umemoto, M. Sano, and K. Chocho, Appl. Phys. Lett. 73 (1998) 832-834.
3. M. Sun, Y. Zhang, X. Gao, and T. Palacios, IEEE Electron Device Lett. 38 (2017) 509-512.
4. T. Palacios, A. Chakraborty, S. Rajan, C. Poblenz, S. Keller, S.P. Denbaars, J.S. Speck, and U.K. Mishra, IEEE Electron Device Lett. 26 (2005) 781-783.
5. S. Keller, N. Fichtenbaum, F. Wu, G. Lee, S.P. Denbaars, J.S. Speck, and U.K. Mishra, Jpn. J. Appl. Physics, Lett. 45 (2006) 322-325.
6. M.H. Wong, S. Keller, N.S. Dasgupta, D.J. Denninghoff, S. Kolluri, D.F. Brown, J. Lu, N.A. Fichtenbaum, E. Ahmadi, U. Singisetti, A. Chini, S. Rajan, S.P. Denbaars, J.S. Speck, and U.K. Mishra, Semicond. Sci. Technol. 28 (2013) 074009.
7. S. Wienecke, B. Romanczyk, M. Guidry, H. Li, E. Ahmadi, K. Hestroffer, X. Zheng, S. Keller, and U.K. Mishra, IEEE Electron Device Lett. 38 (2017) 359-362.
8. B. Romanczyk, S. Wienecke, M. Guidry, H. Li, E. Ahmadi, X. Zheng, S. Keller, and U.K. Mishra, IEEE Trans. Electron Devices 65 (2018) 45-50.
9. F. Akyol, D.N. Nath, E. Gür, P.S. Park, and S. Rajan, Jpn. J. Appl. Phys. 50 (2011) 052101.
10. D. Won, X. Weng, and J.M. Redwing, Appl. Phys. Lett. 100 (2012) 021913.
11. U. Choi, K. Lee, J. Han, T. Jang, Y. Nam, B. So, T. Kwak, and O. Nam, Thin Solid Films 675 (2019) 148-152.
12. F. Yi, N. Xianfeng, X. Jingqiao, N. Biyikli, F. Qian, S. Chevtchenko, Ü. Özgür, H. Morkoç, K. You, R. Devaty,

W.J. Choyke, C.K. Inoki, and T.S. Kuan, MRS Proceedings. 955 (2006) 0955.

13. O. Ambacher, B. Foutz, J. Smart, J.R. Shealy, N.G. Weimann, K. Chu, M. Murphy, A.J. Sierakowski, W.J. Schaff, L.F. Eastman, R. Dimitrov, A. Mitchell, and M. Stutzmann, J. Appl. Phys. 87 (2000) 334-344.
14. A. Meingast, in "Analytical TEM Investigations of Nano-scale Magnetic Materials" (Graz Univertsity of Technology, 2015) 86.
15. J.T. Torvik, M.W. Leksono, J.I. Pankove, C. Heinlein, J.K. Grepstad, and C. Magee, J. Electron. Mater. 28 (1999) 234-239.
16. S. Yamada, J.I. Kato, S. Tanaka, I. Suemune, A. Avramescu, Y. Aoyagi, N. Teraguchi, and A. Suzuki, Appl. Phys. Lett. 78 (2001) 3612-3614.
17. Y. Lin, S. Zhou, W. Wang, W. Yang, H. Qian, H. Wang, Z. Lin, Z. Liu, Y. Zhu, and G. Li, J. Mater. Chem. C 3 (2015) 1484-1490.
18. Z.Y. Al Balushi and J.M. Redwing, J. Mater. Res. 30 (2015) 2900-2909.
19. E. Pitthan, A.L. Gobbi, H.I. Boudinov, and F.C. Stedile, J. Electron. Mater. 44 (2015) 2823-2828.
20. D. Won and J.M. Redwing, J. Cryst. Growth 377 (2013) 51-58.
21. K. Akiyama, Y. Ishii, S. Abe, H. Murakami, Y. Kumagai, H. Okumura, T. Kimoto, J. Suda, and A. Koukitu, Jpn. J. Appl. Phys. 48 (2009) 095505.
22. D. Zhang and Y. Gan, Appl. Surf. Sci. 285 (2013) 211-214.
23. M.A. Reshchikov and H. Morkọ, J. Appl. Phys. 97 (2005) 061301.
24. M.A. Reshchikov, F. Shahedipour, R.Y. Korotkov, B.W. Wessels, and M.P. Ulmer, J. Appl. Phys. 87 (2000) 3351-3354.
25. D. Won, X. Weng, Z.Y. Al Balushi, and J.M. Redwing, Appl. Phys. Lett. 103 (2013) 241908.
26. M.A. Reshchikov, J. Jasinski, Z. Liliental-Weber, D. Huang, L. He, P. Visconti, and H. Morkoç, Phys. B Condens. Matter 340-342 (2003) 440-443.
27. L.T. Romano and T.H. Myers, Appl. Phys. Lett. 71 (1997) 3486-3488.